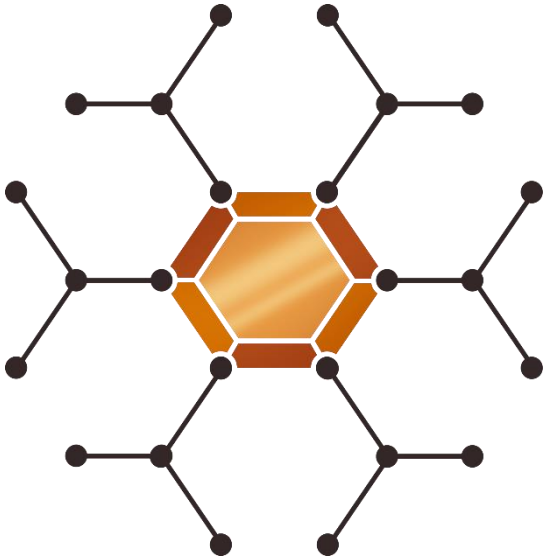

# CLUSTER TWO

## MATERIAL SCIENCE AND TECHNOLOGY

The connected structure surrounding the gemstone represents the promising applications--similar to the potential of graphene--of using existing material, then designing and discovering new compositions and structures, physically and chemically. Meanwhile, the orange color is representative of attraction. In this case, attraction may be used to represent the chemical bonds that can be referred down to the molecular level.

These studies fall under the Industry, Energy, and Emerging Technology (IEET) Research Development Agenda and its aims of developing competitive industries and increased focus on research in order to maximize usage of existing resources.

BASED ON: Harmonized National Research and Development Agenda (HNRDA)

# Comparison in yield of the microwave-assisted method and conventional method in *Zea mays* var. *ceratina* (glutinous corn) cobs cellulose fiber extraction

CAROLYN GRACE C. SACATE, HENDRIK LORENZ B. ALABATA, JASON SANTINO T. ADVINCULA, and XAVIER ROMY O. BRAÑA

*Philippine Science High School Western Visayas Campus - Department of Science and Technology (DOST-PSHSWVC), Brgy. Bito-on, Jaro, Iloilo City 5000, Philippines*

**Article Info**

**Submitted:** May 07, 2021
**Approved:** Jul 13, 2021
**Published:** Aug 30, 2021

***Keywords:***
microwave-assisted
extraction
cellulose
yield
*Zea mays* var. *ceratina*

**Abstract**

Cellulose is a biopolymer that is abundant in nature, often extracted from raw materials via the conventional method. However, a new method of fiber extraction called the microwave-assisted method is said to be cost and energy-efficient. In this study, cellulose fibers were extracted from *Zea mays* var. *ceratina* cobs via microwave-assisted method (MAM) and conventional method (CM), wherein the yield means of the two methods were determined and statistically compared. *Z. mays* cob powder was subjected to 8% (w/v) NaOH for the alkalization process, 5% (w/w) $H_2O_2$ for the acid hydrolysis, and heated using a microwave oven and hot plate for MAM and CM, respectively. The results showed that the MAM and CM yielded 72.7% and 44.6% cellulose fibers, respectively. Statistical analysis via Mann-Whitney U test showed that there is an observed trend towards MAM yielding a higher percentage of crude cellulose in contrast to CM.

**Introduction. -** Cellulose is a biopolymer that is abundant in nature, renewable, and biodegradable, making it a potential industrial material [1]. Synthesized cellulose fibers are utilized in various applications such as in textiles, paper, packaging, building materials, and synthetic fibers [2].

For the past several years, climate change and the additional problems involving agricultural waste urge industries to utilize natural sources instead of synthetic materials. According to Zafar [3], the Philippines is an agricultural country that consists of a land area 30 million hectares wide, wherein 47% of which is utilized in the agricultural sector. Due to this, agricultural residues are also abundant which are common sources of renewable materials and most of them are considered as waste materials. Cobs are by-products derived from *Zea mays*, more commonly known as corn plants. In 2020, the Philippine corn production was about 8.12 million metric tons [4]. Subsequently, the corn cob waste by-product had an estimated technical volume of about 1.95 million metric tons, with most of it being discarded or burnt [5]. This resulted in environmental damages such as global warming due to greenhouse gas emissions (e.g. carbon dioxide, methane) [6,7]. Corn cobs, however, have the potential to become a cheap and abundant raw material for cellulose extraction, as corn cobs are primarily composed of cellulose, hemicellulose, and lignin [2]. The cobs typically have a cellulose fiber content of around 40–44% [8].

Cellulose extraction is the process of isolating cellulose from raw materials or natural fibers. It generally involves the use of alkalis or bisulphites for the treatment of the fibers to isolate lignin and obtain the hemicellulose. There are three primary methods used in extracting cellulose: alkaline treatment, bleaching, and acid hydrolysis [9]. Moreover, cellulose can be extracted using different kinds of methods such as the conventional and microwave-assisted. Every procedure has different pros and cons associated with the yield and properties of the cellulose [10].

The conventional method typically involves the use of instruments that heat the walls of reactants through conduction or convection [11]. Most studies use the conventional method for extracting cellulose fiber because it is simple, effective, and has a high fiber yield [12,13]. However, the process is often slow since it requires high external temperatures to generate the required heat. Furthermore, the rate of the heat flow into the body of the material from the surface limits the process time. Moreover, the heat is also uneven since some parts such as the surface, edges, and corners tend to be hotter in contrast to the interior of the material [11].

Contrasting this, a new method of fiber extraction, called the microwave-assisted method, reportedly yields analytes with higher purity compared to the conventional method [11].

*How to cite this article:*
CSE: Sacate CGC, Alabata HLB, Advincula JST, Braña XRO. 2021. Comparison in yield of the microwave-assisted method and conventional method in *Zea mays* var. *ceratina* (glutinous corn) cob cellulose fiber extraction. Publiscience. 4(1): 27–31.
APA: Sacate C.G.C, Alabata H.L.B., Advincula J.S.T, & Braña X.R.O. (2021). Comparison in yield of the microwave-assisted method and conventional method in *Zea mays* var. *ceratina* (glutinous corn) cob cellulose fiber extraction. *Publiscience*, *4*(1), 27–31.

For supplementary data, contact: publiscience@wvc.pshs.edu.ph.

Microwave heating is an alternative method in extracting bio-based materials due to its capability to accelerate chemical processes. As compared to the conventional method, microwave-assisted method is more rapid and volumetric due to the direct interaction between the material subjected and the heat generated by the applied electromagnetic field. Additionally, it is highly selective, uniform, and utilizes less amount of energy for the pretreatment of bioproducts [2].

With the above information in mind, cellulose from glutinous corn cobs was extracted using the microwave-assisted and conventional methods. The resulting yield obtained from both methods were compared and analyzed using Mann-Whitney U test to determine if a significant difference exists in terms of yield. Microwave-assisted mechanism can be implemented in the production of cellulose obtained from corn cobs, specifically *Zea mays* var. *ceratina,* to address problems such as expensive cost and longer duration of the extraction process, as well as the lack of investigation regarding the comparison of yields between the microwave-assisted and conventional methods.

This research aimed to compare the yields of the microwave-assisted method and conventional method in extracting cellulose fibers from *Zea mays* var. *ceratina* cobs. Specifically, it aimed to:

(i) measure the percent yield of the extracted cellulose fibers from corn (*Z. mays* var. *ceratina*) cobs via microwave-assisted chemical extraction method;

(ii) measure the percent yield of the extracted cellulose fibers from corn (*Z. mays* var. *ceratina*) cobs via conventional method;

(iii) determine a significant difference among yield means of crude cellulose extracted via microwave-assisted and conventional methods, respectively, using Mann-Whitney U test, and;

(iv) qualitatively assess the presence of cellulose in the extracted analytes through the development of a purplish hue upon addition of the Schultze's reagent.

**Methods.** - This study is descriptive in nature. *Z. mays* cobs cellulose fibers were extracted using two extraction methods: microwave-assisted method (MAM) and conventional method (CM). Cellulose fiber extraction is mainly composed of two main processes: alkalization and acid hydrolysis. Ground corn cob powder was subjected to alkalization using sodium hydroxide (NaOH), then followed by acid hydrolysis using hydrogen peroxide ($H_2O_2$). Three replicates per setup were extracted and percentage yield means were calculated. Extraction processes were then followed by the determination of whether the analyte contains cellulose or not using Schultze's reagent. A purplish color upon contact would then signify the presence of cellulose. In determining whether the percentage yield means are significantly different from each other, the non-parametric statistical analysis tool Mann-Whitney U test was used.

*Zea mays Cobs Acquisition, Authentication and Storage.* Glutinous corn cobs (*Z. mays* var. *ceratina*) were purchased and collected from a local corn vendor located in Q. Abeto St., Mandurriao, Iloilo City. Corn variety was authenticated by the Department of Agriculture - Iloilo Research Outreach in Sta. Barbara, Iloilo, to which an official certification was issued.

Acquired corn cobs were washed prior to sun-drying. This is to ensure the safety of the researchers and the residents of the household wherein the study was conducted in. The obtained corn cobs were sundried outdoors for 48 hours to remove moisture. The cobs were also turned every six (6) hours to ensure that every part was evenly dried. The corn cobs were stored in an airtight container and kept in a place away from direct sunlight at room temperature to prevent dry matter loss during nighttimes, prior to usage [14].

*Zea mays Cob Preparation.* Corn cobs were pulverized into fine powder using a blender (Moulinex Turbo Blender). The powder was then sieved using a fine mesh sieve (pore size: 841 µm). Larger particles were reground using a mortar and pestle to enable passage through the sieve. The powder used for all treatments was a mixture of all grounded cobs. Powdered samples were dried in an oven (La Germania SL6031-21) at 135 °C until a constant weight was achieved. Constant weight was determined through the continuous drying and hourly weighing of samples until two consecutive weighings did not differ by more than 0.5 mg per gram of the sample initially taken [15]. Prior to the hourly weighing of heated samples, samples were cooled to room temperature. Ten (10) grams of *Zea mays* var. *ceratina* powder from each replicate were then placed inside airtight containers. They were then stored at room temperature until further use.

*Cellulose Extraction via Microwave-assisted Method.* Microwave heating was conducted in a 2450 MHz microwave oven (Hanabishi HMO-17M-3), wherein the power per microwave-assisted heating was set to 500W, three (3) minutes per replicate [2,16].

The corn cob powder samples underwent alkalization using NaOH as the alkaline treatment, wherein ten (10) grams of the corn cob powder was added into 150 mL 4% (w/v) NaOH, then subjected to microwave heating with the specified settings. The acquired corn cob pulp was washed with distilled water until neutral pH (around 6.5–8) was acquired, measured using pH test strips [16,17]. After the alkalization process, acid hydrolysis was performed. Here, the alkalized corn pulp was bleached in 50 mL 5% (w/w) $H_2O_2$ solution. The pulp was then subjected to microwave heating following the same settings stated above. Extracted cellulose fibers were then rewashed until neutral pH was acquired. To rid the analyte of water, it was dried using the oven until a constant weight was achieved [2,18]. Three (3) replicates were used in this step.

*Cellulose Extraction via Conventional Method.* Corn cob powder was subjected to alkalization then

heated using a hot plate equipped with a temperature reader (Biobase MS7-NS50-Pro), wherein the beaker with the alkaline treatment was placed on the hot plate set at 100 °C for four (4) hours with constant stirring. After washing until neutral pH was acquired, the pulp was then submerged and hydrolyzed in the $H_2O_2$ solution. Extracted cellulose fibers were then subjected once more to washing until neutral pH was acquired. To rid the analyte of water, the analyte was dried using the oven until a constant weight was achieved [18]. Three (3) replicates were used in this step.

*Qualitative Determination of Presence of Cellulose using Schultze's Reagent.* Extracted cellulose fibers were assessed qualitatively using Schultze's reagent to determine the presence of cellulose in the extracted analyte. In preparing the reagent, twenty (20) grams of zinc chloride ($ZnCl_2$) was dissolved in 9.5 mL warm distilled water then cooled. On a separate beaker, 0.5 g iodine and 1 g potassium iodide were dissolved in 20 mL deionized water, wherein 1.5 mL of this solution was added to the zinc chloride solution until a persistent precipitate of iodine formed. Direct contact of the Schultze's reagent to cellulose fibers would yield a purplish color [19,20].

*Computation of Percentage Yield.* In the computation of percentage yield, the following formula was used:

$$\%yield = \frac{acquired\ dry\ mass\ of\ cellulose\ fibers\ (g)}{dry\ mass\ of\ raw\ material\ used\ (g)} \times 100$$

The mean percent cellulose fiber yields were then calculated. The calculated mean—one for each method—served as the overall percentage of cellulose fiber yield.

*Data Analysis.* Mann-Whitney U test was utilized in determining whether the percentage yield means are significantly different from each other, wherein in this process, the equation function of Microsoft® Excel® for Microsoft 365 MSO (16.0.13929.20360) 64-bit. The data would be then deemed significantly different if $p<0.05$ [21].

*Safety Procedure.* A Materials Safety Data Sheet (MSDS) was secured and provided beforehand wherein hazards regarding the conduct of this study were determined. Mitigation of these hazards were subsequently observed and implemented. Laboratory protective gear consisting of laboratory gowns, gloves, and masks were worn at all times during the conduct of the study.

**Results and Discussion.** - Crude cellulose fibers were extracted from *Zea mays* var. *ceratina* cobs via MAM and CM. Schultze's agent was then added to the extracted analyte to determine the presence of cellulose. The resulting purple hue signified that the extracted analyte contains cellulose. This is shown in Figure 1. However, a greenish hue was also observed, signifying the presence of non-cellulosic material such as lignin.

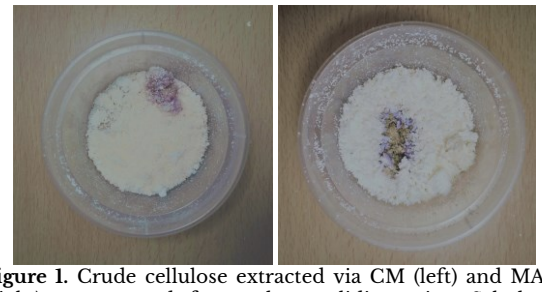

**Figure 1.** Crude cellulose extracted via CM (left) and MAM (right) were tested for analyte validity using Schultze's reagent, to which the purplish color indicated the presence of cellulose.

Furthermore, the crude cellulose extracted via MAM are higher in contrast to the ones extracted via CM, as shown in Table 1. Additionally, replicate yields and means per setup along with their respective standard deviations are presented in Figure 2.

**Table 1.** The table below shows the percentage yield means and medians per setup.

| Setup | Yield mean (%) | Yield median (%) |
|---|---|---|
| MAM | 72.7 | 72.0 |
| CM | 44.6 | 42.0 |

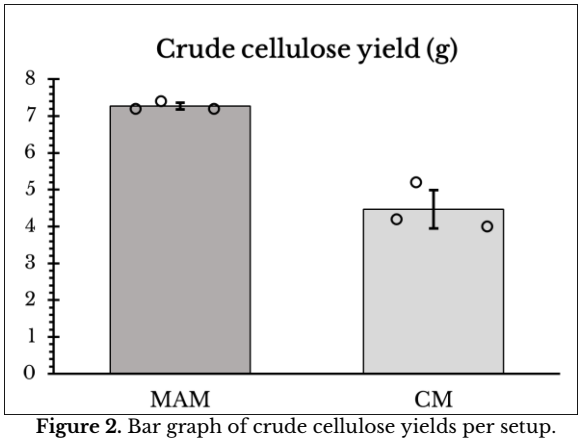


**Figure 2.** Bar graph of crude cellulose yields per setup.

The higher crude cellulose yield through MAM extraction may be attributed to the uniformity of heat generated by the emitted low-frequency radiation of the microwave [17]. Reactants and solvents are heated rather than the container itself as the radiation passes through the walls of the container, exciting the polar molecules within the substance being heated. Heat is generated through the movement of these polar molecules. This leads to less by-products and decomposition products which enabled the increase of the yield percentage [17,22].

In contrast, heating using CM is prone to temperature gradient which results in overheating and eventually product decomposition leading to a lower yield percentage [22]. The 2015 study of Garadimani et al. [23], which used the conventional method of extraction, found that the extraction of *Z. mays* cobs cellulose fibers yielded a mean of 41.5% of cellulose. In terms of yield, this is close to the findings of the current study using the same method.

Calculations showed that the p-value of the data acquired from both extraction methods is 0.049535. Though less than the significance level of 0.05, a clear significant difference is not apparent; therefore, the p-value only signifies a trend towards MAM extracting a higher amount of crude cellulose in contrast to CM.

*Limitations.* Due to time and resource constraints, this study only compared the methods based on only one parameter. This is due to the lack of equipment as the study was conducted during a pandemic.

**Conclusion.** - Findings show that the MAM and CM were able to extract 72.7% and 44.6% of crude cellulose, respectively. The purple hue that developed upon the addition of Schultze's reagent signifies the presence of cellulose. However, the development of a greenish hue signifies the presence of non-cellulosic material within the extracted analytes. Through statistical analysis, it was determined that there is an observed trend towards the microwave-assisted method yielding a higher percentage of *Zea mays* var. *ceratina* crude cellulose in contrast to the conventional method.

**Recommendations.** - Future related studies are recommended to include more parameters such as thermal stability, morphology, and crystallinity for comparison of MAM and CM [2]. Moreover, in contrast to the Schultze's reagent, the usage of the Van Soest Analysis would provide a quantitative result with regards to analyte purity [24,25]. Furthermore, future studies are recommended to explore more on the non-thermal effects of microwave heating as well as the effects of microwave heating modes (e.g. intermittent, continuous) in biopolymer extraction from raw materials.

**Acknowledgment.** - Gratitude is extended to Ms. Ma. Carmen Primitiva B. Malaga of the Department of Agriculture-Iloilo ROS for authenticating the corn cob samples, and to Mrs. Corazon Jotas for supplying the cobs.

**References**

[1] Saragih SW, Wirjosentono B, Eddyanto, Meliana Y. 2019. Extraction and Characterization of Cellulose from Abaca Pseudo Stem (Musa textile). J Phys Conf Ser. 1232:012018. doi: 10.1088/1742-6596/1232/1/012018.

[2] Li M, Cheng YL, Fu N, Li D, Adhikari B, Chen XD. 2014. Isolation and characterization of corncob cellulose fibers using microwave-assisted chemical treatments. Int J Food Eng. 10(3): 427–436. doi: 10.1515/ijfe-2014-0052.

[3] Zafar S. 2020 Jul 23. Agricultural wastes in the Philippines. Bioenergyconsult.com. [accessed 2020 Oct 24]. Available from: https://bit.ly/3ftZloE.

[4] Philippine Statistics Authority. 2021. Palay and Corn Production Survey. [accessed 2021 Mar 13]. Available from: https://bit.ly/3fSScwR.

[5] Caparino, O. A., PhD. 2018 Feb 22. Status of Agricultural Waste and Utilization in the Philippines. [accessed 2020 Nov 26]. Available from: https://bit.ly/3yNvdfl.

[6] Berber-Villamar NK, Netzahuatl-Muñoz AR, Morales-Barrera L, Chávez-Camarillo GM, Flores-Ortiz CM, Cristiani-Urbina E. 2018. Corncob as an effective, eco-friendly, and economic biosorbent for removing the azo dye Direct Yellow 27 from aqueous solutions. PLoS One. 13(4): e0196428. doi:10.1371/journal.pone.0196428.

[7] Romasanta RR, Sander BO, Gaihre YK, Alberto MC, Gummert M, Quilty J, Nguyen VH, Castalone AG, Balingbing C, Sandro J, et al. 2017. How does burning of rice straw affect$CH_2$ and $N_2O$emissions? A comparative experiment of different on-field straw management practices. Agric Ecosyst Environ. 239:143–153. doi: 10.1016/j.agee.2016.12.042.

[8] Wang Y, Hu Y, Qi P, Guo L. 2019. A new approach for economical pretreatment of corncobs. Applied Sciences (Basel, Switzerland), 9(3), 504. doi: 10.3390/app9030504.

[9] Johar N, Ahmad I, Dufresne A. 2012. Extraction, preparation and characterization of cellulose fibres and nanocrystals from rice husk. Ind. Crops Prod. 37: 93–99. doi: 10.1016/j.indcrop.2011.12.016.

[10] Moran JI, Alvarez VA, Cyras VP, Vasquez A. 2007. Extraction of cellulose and preparation of nanocellulose from sisal fibers. Cellulose. 15: 149–159. doi: 10.1007/s10570-007-9145-9.

[11] Zhu YJ, Chen F. 2014. Microwave-assisted preparation of inorganic nanostructures in liquid phase. Chem. Rev. 114(12): 6462–6555. doi: 10.1021/cr400366s.

[12] Yilmaz ND. 2013. Effect of chemical extraction parameters on corn husk fiber characteristics. Indian J Fibre Text Res. 38: 29–34. Available from: https://bit.ly/3fveupO.

[13] Naili, H., Jelidi, A., Limam, O., Khiari, R. 2017. Extraction process optimization of Juncus plant fibers for its use in a green composite. Ind Crops Prod. 107: 172–183. doi: 10.1016/j.indcrop.2017.05.006.

[14] Del Campo BG, Brumm TJ, Bern CJ, Nyendu GC. 2014. Corn Cob Dry Matter Loss in Storage as Affected by Temperature and Moisture Content. Agricultural and Biosystems Engineering Publications. 57(2): 573–578. doi: 10.13031/trans.57.10426.

[15] General Notices and Requirements: Applying to Standards, Tests, Assays, and Other Specifications of the United States Pharmacopeia. 2013 Feb 1. [accessed 2020 Nov 22]. Available from: https://bit.ly/3i03wu3.

[16] Camani PH, Anholon BF, Toder RR, Rosa DS. 2020. Microwave-assisted pretreatment of eucalyptus waste to obtain cellulose fibers. Cellulose. 27(7): 3591–3609. doi: 10.1007/s10570-020-03019-7.

[17] Izgi AA, Kocak ED, Sahinbaskan BY. 2018. Microwave Assisted Surface Treatment of Okra Fibers. IOP Conf Ser Mater Sci Eng. 460 012042. doi: 10.1088/1757-899X/460/1/012042.

[18] Hernando, K., Abayon, M., Sitjar, J., Aguirre, M., Catolico, J. 2019. Characterization of the Physical Properties of Bacillus thuringiensis Corn husk Fibers through Alkalization. Publiscience. 1(1): 2–7. Available from: https://bit.ly/2SzEs2b.

[19] Elfick, J. 2020 May 15. *School Science Lessons - Appendix B*. [accessed 2020 Oct 22]. Available from: https://bit.ly/2TpXEQt.

[20] Jenkin, A., Jenkin, D. 2012. *Sugar, starch or cellulose? What sort of carbohydrates do plants make?* [accessed 2020 Oct 22]. Available from: https://bit.ly/3vveMSR.

[21] Zach. 2020 Mar 24. How to perform a Mann-Whitney U test in Excel. Statology.org. [accessed 2020 Dec 5]. Available from: https://bit.ly/3uuRKKH.

[22] Lidstrom P, Tierney J, Wathey B, Westman J. 2001. Microwave assisted organic synthesis - a review. *Tetrahedron. 57*(45): 9225–9283. doi: 10.1016/S0040-4020(01)00906-1.

[23] Garadimani KR, Raju GU, Kodancha KG. 2015. Study on Mechanical Properties of Corn Cob Particle and E-Glass Fiber Reinforced Hybrid Polymer Composites. Am J Mater Sci. 5(3C): 86–91. doi: 10.5923/c.materials.201502.18.

[24] Holtzapple MT. 2003. CELLULOSE. *Encyclopedia of Food Sciences and Nutrition.* 998–1007. doi:10.1016/b0-12-227055-x/00185-1.

[25] Wichern M, Gehring T, Lübken M. 2018. Modeling of biological systems in wastewater treatment. In: Reference Module in Earth Systems and Environmental Sciences. Elsevier. doi: 10.1016/B978-0-12-409548-9.10944-3.

Publiscience Vol. 4 Issue 1

# Development of a reduced nanoporous graphene oxide membrane synthesized from *Oryza sativa* husk using the Tour method for the reduction of salt ions

VENN DEO JUSTIN E. ALBALADEJO[1], RAYMOND T. BORRES[1], ZEDDREX N. NAVARRA[1], ARIS C. LARRODER[1], and MARK V. ROSALES[2]

[1]*Philippine Science High School Western Visayas Campus - Department of Science and Technology (DOST-PSHSWVC), Brgy. Bito-on, Jaro, Iloilo City 5000, Philippines*
[2]*Metrology Laboratory, Regional Standards, and Testing Laboratories, Lapaz, Iloilo City 5000, Department of Science and Technology, Philippines*

**Article Info**

**Submitted:** Apr 19, 2021
**Approved:** Jun 24, 2021
**Published:** Aug 30, 2021

***Keywords:***
graphene oxide
nanoporous membrane
Tour method
*Oryza sativa*
desalination

**Abstract**

Membrane desalination is limited by issues of high costs and energy consumption. Moreover, high-quality membranes require high carbon content sources such as biowastes, among others. One example of biowastes commonly found in the Philippines are *Oryza sativa* (rice) husks. Thus, this study aimed to determine the feasibility of developing a reduced nanoporous graphene oxide (rNPGO) membrane synthesized from *Oryza sativa* husks using the Tour method for membrane desalination. To assess the membrane, a salt solution (1% w/v) was prepared and subjected to membrane desalination. After three readings, the recorded mean salt rejection rate of the membrane was 6.55%. The results indicate a significant difference between the salinity content before and after desalination. Therefore, rNPGO synthesized from *O. sativa* husks using the Tour method can be used for the reduction of salt ions.

**Introduction.** - Membrane desalination is a process that removes salt ions from saltwater with the use of membranes [1,2,3]. Recent developments in the field of membrane desalination have led it to become one of the primary solutions to address saltwater intrusion [1,3]. Saltwater intrusion is a form of groundwater contamination wherein saltwater intrudes into freshwater sources, making it unsuitable for human consumption. By removing the salt ions in the water, membrane desalination provides the possibility of expanding the water supply by supplementing it with water from oceans and brackish waters [4].

However, the current leading technologies for membrane desalination are limited in part due to high costs and energy consumption [2]. One of the causes of the elevated operating costs is the presence of membrane fouling, which is the degradation of the membrane due to the deposition of permeate molecules on the surface [5]. This leads to the deterioration of permeate flux, frequent chemical cleaning, and replacement of the membrane, contributing to a shorter membrane lifespan [6,7].

In a study conducted by Wang et al. [7], graphene-based membranes can withstand membrane fouling. Graphene is an ultra-thin carbon film that contains a honeycomb lattice structure which gives it a large surface area and excellent conductivity [8]. Additionally, graphene-based membranes can withstand membrane fouling due to their hydrophilic nature as well as their strong adsorption capacity and large surface area [9].

Moreover, the introduction of nanopores to graphene-based membranes causes an increase in permeate flux while maintaining a relatively high salt rejection rate [4,10,11]. Additionally, graphene-based nanoporous membranes are commonly utilized in membrane desalination because of their attractive properties to salt ions [11], and effective nanopore filtration [12]. The attractive properties of graphene-based nanoporous membranes to salt ions derive from the Gibbs-Donnan effect wherein negatively charged membranes such as graphene-based nanoporous membranes attract positively charged molecules such as sodium ions. Furthermore, due to the size difference between nanopores and salt ions, salt ions are unable to pass through nanopores that are under a certain size [13].

Since nanoporous graphene oxide (NPGO) membranes are chemically unstable due to the presence of oxygen-containing functional groups, they must be stabilized through thermal reduction. Thermal reduction is a controlled approach to removing the oxygen-containing functional groups

*How to cite this article:*
CSE: Alabaldejo VDJE, Borres RT, Navarra ZN, Larroder AC, Rosales MV. 2021. Development of a reduced nanoporous graphene oxide membrane synthesized from Oryza sativa husk using the Tour method for the reduction of salt ions. Publiscience. 4(1): 32–37.
APA: Alabaldejo, V.D.J.E., Borres, R.T., Navarra, Z.N., Larroder, A.C., & Rosales, M.V. (2021). Development of a reduced nanoporous graphene oxide membrane synthesized from Oryza sativa husk using the Tour method for the reduction of salt ions. *Publiscience*, *4*(1), 32–37.

For supplementary data, contact: publiscience@wvc.pshs.edu.ph.

in the NPGO membranes, which increases membrane permeability, uniformity, and stability [13].

When synthesizing a graphene oxide (GO) membrane, the quality of the resulting membrane is dependent on the quality of the graphite used in its synthesis. Hence, in order to obtain high-quality membranes, high carbon content sources are necessary. One example of sources with high carbon content are biomasses such as rice husks, among others [7,14,15]. In the study conducted by Supriyanto et al. [16], promising results were obtained for the synthesis of GO from graphite that had been obtained from *O. sativa* (rice) husk.

The two main methods used for the synthesis of GO are the Tour method and Hummer's method. However, in the study of Habte and Ayele [17], the Tour method was shown to have a clear advantage in the synthesis of GO in comparison to the Hummer's method. This is because the oxidation degree of the synthesized GO was found to be better when the Tour method is used. The higher oxidation degree implies that the attractive filtration property of the membrane was stronger and therefore increased the salt rejection rate of the membrane. Additionally, the presence of health risks and hazards when synthesizing the GO was reduced when the Tour method is utilized because it minimizes the fumes released during the process in contrast with Hummer's Method.

Therefore, the study aimed to explore the feasibility of developing a reduced nanoporous graphene oxide membrane (rNPGO) synthesized from rice husk using the Tour method to reduce salt ions. It specifically aimed to:

(i) synthesize graphite from *O. sativa* husk;

(ii) synthesize graphene oxide from graphite using the Tour method;

(iii) etch nanopores in the graphene oxide powder;

(iv) prepare and reduce the NPGO membrane; and

(v) assess the salinity level of the water samples pre and post-desalination using the rNPGO membrane.

**Methods.** - *Oryza sativa* husks were gathered from the Department of Agriculture - Western Visayas Agricultural Research Center and synthesized into graphite. The graphite was then synthesized into graphene oxide using the Tour method. Subsequently, nanopores were etched into the graphene oxide. After the preparation of the membrane, a salt solution was prepared and measured based on its salinity content. It was then filtered using the membrane and the salinity content of the permeate was measured.

*Synthesis of Graphite.* The synthesis of graphite was needed to make a graphene oxide membrane. The graphite powder for this research was derived from *O. sativa* husks. The rice husks (500 g) were washed with distilled water and subjected to oven-drying for 24 hours in different batches at 50°C. The material produced was then ground and screened using a sieve mesh size 60 (0.250 mm). A hundred grams of the rice husk residue was placed in a furnace at 1000 °C for 2 hours, under 1 atm. To obtain graphite, silica was removed from the furnaced rice husk using 4 M sodium hydroxide (NaOH) that was pre-diluted in a volumetric flask. This was done by dissolving 10 g of the furnaced rice husk in 30 mL of 4 M NaOH in a flask which was then heated and stirred for 3 hours. The solution was then vacuum-filtered and oven-dried for 3 hours at 50 °C. The resulting graphite underwent a confirmatory test using the Fourier-Transform Infrared Radiation - Attenuated Total Reflectance (FTIR-ATR) to confirm if the synthesized material is indeed graphite by comparing it with the FTIR-ATR spectroscopy results of related literature.

*Synthesis of Graphene Oxide using the Tour Method.* Ninety milliliters (90 mL) of concentrated 98% sulfuric acid ($H_2SO_4$) was mixed in a glass beaker with 10 mL of concentrated 85% phosphoric acid ($H_3PO_4$). The mixture was poured into a beaker with a mixture of 0.5 g of graphite powder and 4.5 g of potassium permanganate ($KMnO_4$), heated at 50 °C using a water bath, and stirred for 12 hours. The mixture was then cooled at room temperature and 250 mL distilled water was added. Ten milliliters (10 mL) of 30% hydrogen peroxide ($H_2O_2$) was added to reduce the manganese ions present. The resulting solution was filtered using a 45 microns filter paper. The produced graphite oxide filter cake was washed using a 5% hydrochloric acid (HCl) (aq) in a centrifuge at 4000 rpm for 4 hours. The GO was then manually stirred with distilled water at 60 °C for 12 hours in a water bath [17]. The solution was vacuum-filtered and oven-dried to produce GO powder which was tested using the FTIR-ATR to confirm if the synthesized material is indeed GO.

*Etching of GO.* Thirty milligrams (30 mg) of GO powder was redispersed into 90 mL of 30% hydrogen peroxide and placed in an ultrasonic bath treatment for 20 minutes to ensure a good dispersion. After 20 minutes, the solution was heated up to 70 °C in a water bath and was refluxed in a reflux set-up for 10 hours. The mixture was purified in a permeable plastic bag with deionized water for 3 days to obtain a stable NPGO solution. The NPGO was diluted to 50 mg/L using deionized water for membrane preparation.

*Preparation of NPGO membrane.* An NPGO membrane was prepared using vacuum filtration. The NPGO solution was filtered by using a filter paper with a pore size of 45 microns to remove the moisture. The filtered NPGO sheet was poured from the Buchner flask to the beaker, vacuum-filtered, and dried in an oven at 60 °C for 12 hours. Then, it was thermally reduced in an oven at 150 °C at 1 atm for 1.5 hours to maximize salt rejection to synthesize an rNPGO membrane. The surface and cross-sectional morphology of the rNPGO membrane was characterized using Scanning Electron Microscopy (SEM). The membrane was captured and the pores in

the resulting image were measured using the 2D image of the result from the SEM Imaging.

*Assessment of salinity content.* To measure and evaluate the efficiency of the rNPGO membrane, an assessment of the salinity level of water samples was conducted. A salt solution was prepared using one gram of analytical reagent grade sodium chloride (NaCl) to make a 1% NaCl solution. Prior to testing the membrane, a control made of a blank filter paper was utilized. The salt solution was poured on top of the filter paper until the funnel was full. The permeate was then placed in a 250 mL beaker for salinity content testing. A conductivity meter, pre-calibrated by dipping it in a container filled with distilled water, was used by dipping it in the solution until the value stabilized after three minutes. For the final testing, the same method was then utilized for the rNPGO membrane.

The salt rejection of the membrane was analyzed using the salinity content of both the feed and the permeate. After all the data were plotted, data analysis was using the formula for salt rejection.

$$R_{salt\%} = \left(1 - \frac{C_p}{C_f}\right) * 100\%$$

Where:
$R_{salt\%}$ = percent of salt rejection
$C_p$ = concentration of the permeate
$C_f$ = concentration of the feed

*Data Analysis.* The results were analyzed using t-test for dependent samples using RStudio (version 1.3.1093.0, free license) to observe any significant difference between the salinity content before and after desalination. The salt rejection was analyzed among the three replicates. This was to ensure that the efficiency of the membrane was not reduced by washing it with deionized water.

*Safety Procedures.* During the conduct of the data gathering process, the wearing of the proper personal protective equipment such as gloves, masks, and goggles was observed. The methods were conducted alongside the supervision of experts. A wash bottle was utilized in cleaning the glassware and the contaminants in the conductivity meter to ensure accurate readings. Furthermore, the safety data sheet of each chemical and equipment was strictly followed. Additionally, when performing methods with the use of chemicals, a fume hood was utilized to avoid the inhalation of fumes. Lastly, for the disposal of chemicals, each chemical was disposed of according to the safety data sheet and in accordance with the disposal protocol of the laboratory.

**Results and Discussion.** - This study aimed to explore the feasibility of developing an rNPGO membrane synthesized from *O. sativa* husk using the Tour method to reduce salt ions. This was done through membrane assessment by analyzing its pore size, membrane thickness, and salt rejection rate.

The graphite powder synthesized from rice husk was analyzed using the FTIR-ATR analysis with three replicates. The mean result of the FTIR-ATR analysis of the graphite powder, colored in red, was compared with the FTIR-ATR results of the graphite powder in the study of Wenxuan et al. [18], colored in black (Figure 1). Since a graphite library was unavailable in the FTIR-ATR used, the graphs were superimposed and the peaks were compared. The peaks of both graphs are similar, which peaks at around 624.38/cm, 790.75/cm, and 1066.50/cm.

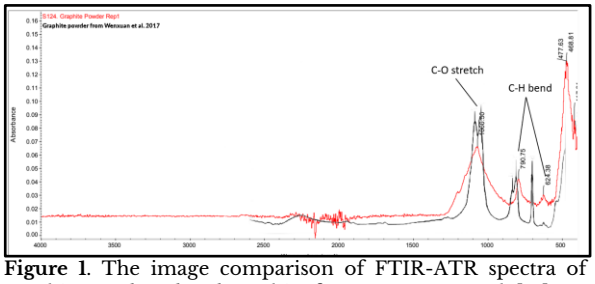


**Figure 1**. The image comparison of FTIR-ATR spectra of graphite produced and graphite from Wenxuan et al. [18].

The graphene oxide powder synthesized using the Tour method was analyzed using the FTIR-ATR analysis with three replicates. The mean result of the FTIR-ATR analysis of the graphene oxide powder, colored in red, was compared to the FTIR-ATR results of the graphene oxide powder in the study of Çiplak et al. [19] colored in blue (Figure 2). The peaks of both graphs which peaks at around 791.67/cm and 1070.04/cm are similar.

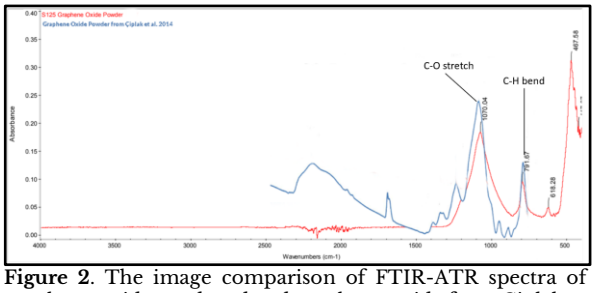


**Figure 2**. The image comparison of FTIR-ATR spectra of graphene oxide produced and graphene oxide from Çiplak et al. [19].

Using an SEM, the rNPGO was analyzed for its pore size and thickness. The nanopore sizes were measured from three different locations and different magnifications respectively on the rNPGO membrane. This was done so that the pores are visible with the use of the instrument. The statistical mean pore sizes of the three replicates are 555.4 nm, 615.1 nm, 837.9 nm respectively. Moreover, the pores have varying sizes that range from 286.0 nm to as large as 1920.0 nm (Table 1).

**Table 1**. Statistical parameters of rNPGO membrane pore sizes based on the 3 locations with 3 magnifications (8500x, 5000x, 3000x).

| Parameters | Replicate at 8500x (nm) | Replicate at 5000x (nm) | Replicate at 3000x (nm) |
|---|---|---|---|
| Statistical Mean | 555.4 | 615.1 | 837.9 |
| Standard Deviation | 323.9 | 372.7 | 413.6 |

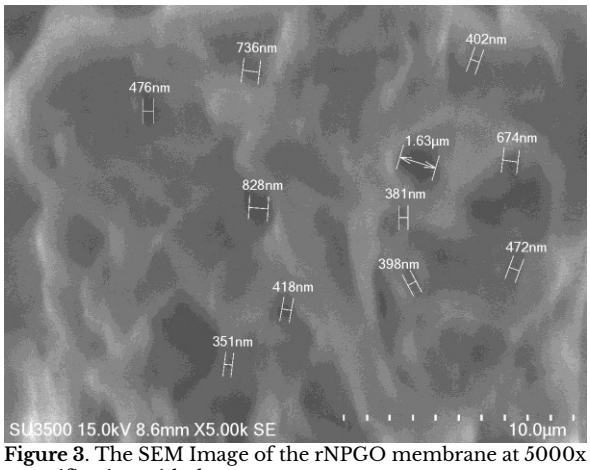


**Figure 3**. The SEM Image of the rNPGO membrane at 5000x magnification with the pore measurements.

The thicknesses of the rNPGO membrane were measured from three different locations and different magnifications respectively. This was done so that the rNPGO membrane was visible enough to measure its thickness with the use of the instrument. The mean thickness, as well as the standard deviation from the three replicates, varies as shown (Table 2). The statistical means of the three replicates are 37.33 µm, 33.19 µm, and 45.43 µm, respectively. Additionally, the thickness of the membrane varies from a range of 27.0 µm to 53.6 µm.

**Table 2.** The statistical parameters of nanoporous graphene oxide membrane thickness based on the 3 locations with 3 magnifications (420x, 370x, 250x).

| Parameters | Replicate at 420x (µm) | Replicate at 370x (µm) | Replicate at 250x (µm) |
|---|---|---|---|
| Statistical Mean | 37.73 | 33.19 | 45.43 |
| Standard Deviation | 3.66 | 4.98 | 4.75 |

The mean salinity content of the prepared salt solution was measured using a conductivity meter (PS-2230 Advanced Water Quality Sensor). The salinity content of both pre-desalination and post-desalination were further analyzed using the Salt Rejection Rate formula. Additionally, the statistical mean and standard deviation were calculated (Table 3).

**Table 3.** The statistical parameters of pre-desalination and post-desalination salinity content of the water samples.

| Replicates | Pre-Desal-ination Salinity Content (%) | Post-Desal-ination Salinity Content (%) | Salt Rejection Rate (%) |
|---|---|---|---|
| 1 | 1.04479815 | 0.96423745 | 7.710647267 |
| 2 | 1.04164610 | 0.98627760 | 5.315480949 |
| 3 | 1.03442845 | 0.96588000 | 6.626698057 |
| Statistical mean | 1.04029090 | 0.97213168 | 6.551938501 |
| Standard deviation | 0.00434051 | 0.01002512 | 0.979288738 |

The FTIR-ATR spectra results showed that the graphite powder produced is similar to the graphite produced in the study of Wenxuan et al. [18], thus, it is feasible to synthesize graphite powder from *O. sativa* husks. The graphs of the FTIR-ATR spectra can be presented in two ways, wavelength vs. transmittance and wavelength vs absorbance. In the study of Wenxuan et al. [18], they utilized wavelength vs transmittance which in turn caused the graph to be reflected based on Beer-Lambert's Law as stated in the study of Mayerhöfer et al. [20].

To determine the feasibility of synthesizing graphite powder from *O. sativa* husk, the reflected graph was compared to the study of Wenxuan et al. [18] based on its fingerprint region. With this, it reflected the result of the study of Supriyanto et al. [16] wherein they also utilized *O. sativa* husk to synthesize graphite.

The FTIR-ATR spectra results showed that the graphene oxide powder produced is similar to the graphite produced in the study of Çiplak et al. [19]. Thus, it is feasible to synthesize graphene oxide powder from graphite using the Tour method. In the study of Çiplak et al. [19], they also utilized the wavelength vs transmittance which in turn caused the graph to be reflected based on Beer-Lambert's Law as stated in the study of Mayerhöfer et al. [20]. To determine the feasibility of synthesizing graphene oxide powder from *O. sativa* husk, the reflected graph was compared to the study of Çiplak et al. [19] based on its functional groups. The graph of the graphene oxide produced has two visible peaks within the fingerprint region of the spectra. By comparing the graphs in this region, it could help indicate if the product is similar to another.

The results obtained from the SEM showed that the graphene oxide membrane produced pore sizes ranging from as small as 286 nm to as large as 1920 nm. Although these are hundreds of nm in diameter, these could not be considered nanopores. This is probably because the nanopores could not be seen by the instrument used since the sample was not sputter-coated beforehand.

The rNPGO membrane was subjected to an SEM imaging analysis at 15 kV settings so that the membrane will not burn. The morphology was analyzed and the measured pores vary in size with a standard deviation of 323.9 nm, 372.7 nm, and 413.6 nm. The deviation between the pore sizes may also be due to the dispersion of the hydrogen peroxide with the graphene oxide powder in a plastic sheet instead of a cellulose dialysis bag as well as the placement of the bag during the stabilization phase [13]. To visualize the pore sizes smaller than 200 nm in size the membrane could have been sputter-coated with gold or analyzed using Atomic Force Microscopy.

Additionally, the results for the SEM imaging of the thickness of the membrane showed that a membrane was prepared onto the filter paper. The thickness of the membrane ranges from 27.0 μm to 53.6 μm which shows the uneven distribution of the membrane probably due to the process of uneven vacuum filtration of the NPGO solution. In addition, this assumption is also reflected by the standard deviation of the membrane thickness which are 3.66 μm, 4.98 μm, and 4.75 μm.

Furthermore, membrane desalination using rNPGO synthesized from *O. sativa* husk has resulted in a mean salt rejection rate of 6.55% and a significant difference between the pre-desalination and post-desalination salinity content. This was done through a t-test for dependent samples ($\alpha$=0.05) and a p-value of 0.011. This shows that the rNPGO membrane developed and synthesized from *O. sativa* husks using the Tour method was capable of reducing salt ions.

The filtration of salt ions can potentially prove that the pore size of the graphene oxide can be considered as nanopores since it was able to reduce the salt ions in the water sample. This is because the attractive properties of graphene-based nanoporous membranes to salt ions are derived from the Gibbs-Donnan effect wherein negatively charged membranes such as graphene-based nanoporous membranes attract positively charged molecules such as salt ions. Furthermore, it can potentially prove that the pore size is nanoporous due to the size difference between nanopores and salt ions. Salt ions are unable to pass through nanopores that are under a certain size since salt ions have a size that is considered nanoparticles. This was reflected in the results when the NPGO membrane was tested for its salt rejection rate and permeate flux and compared with the results of a graphene oxide membrane [13].

*Limitations.* The FTIR-ATR results did not directly indicate that the sample is graphite due to the graphite library unavailability for the FTIR-ATR utilized. Additionally, the *O. sativa* husks did not undergo vacuum furnacing, one of the ideal methods for synthesizing graphite from biomass. Lastly, the removal of silica was not conducted using hydrofluoric acid (HF), which is better for removing silica than NaOH in terms of purity.

**Conclusion.** In this study, the feasibility of developing a rNPGO synthesized from *O. sativa* husk using the Tour method was explored. The FTIR-ATR results of both the graphite powder and graphene oxide powder indicated the feasibility of synthesizing graphene oxide powder using the Tour method from the graphite powder synthesized from rice husk. The membrane produced contained pores etched in the graphene oxide powder. Moreover, there is a significant difference in the salinity content of the pre-desalination and post-desalination water samples after undergoing desalination using the nanoporous graphene oxide membrane. Thus, a nanoporous graphene oxide membrane was developed and synthesized from *O. sativa* husk using the Tour method.

**Recommendations.** - The sample could be placed in a polyethersulfone filter and sputter-coated to better visualize the nanopores of the graphene oxide using an SEM. Atomic Force Microscopy could also be utilized for better magnification in the sample. Additionally, the salt load capacity of the membrane could be assessed by desalinating the sample multiple times. This study can be a step further towards the right direction for exploring new avenues for the use of biowastes such as *O. sativa* husk that is abundant in the Philippines. However, there is still a lot of room for improvement in the desalination aspect of a reduced nanoporous graphene oxide (rNPGO) membrane derived from *O. sativa* husk before it can be used as a solution to the saltwater intrusion in coastal areas in the Philippines.

**Acknowledgment.** - The researchers would like to extend their gratitude to NEDA Region VI for helping in the conceptualization of the research problem, Mr. Roxzien Sesbreño for facilitating their data gathering at DOST-VI, and Mrs. Jessebel V. Gadot for facilitating the data gathering at UPV-RRC.

**References**

[1] Abd-Elhamid HF, Javadi AA. 2011. A Cost-Effective Method to Control Seawater Intrusion in Coastal Aquifers. Water Resources Management. 25(11): 2755–2780. doi: 10.1007/s11269-011-9837-7.

[2] Shaffer DL, Yip NY, Gilron J, Elimelech M. 2012. Seawater desalination for agriculture by integrated forward and reverse osmosis: Improved product water quality for potentially less energy. Journal of Membrane Science. 415-416: 1–8. doi: 10.1016/j.memsci.2012.05.016.

[3] Mehdizadeh S, Badaruddin S, Khatibi S. 2019. Abstraction, desalination and recharge method to control seawater intrusion into unconfined coastal aquifers. Global Journal of Environmental Science and Management. 5(1): 107–118.

[4] Cohen-Tanugi D, Mcgovern RK, Dave SH, Lienhard JH, Grossman JC. 2014. Quantifying the potential of ultra-permeable membranes for water desalination. Energy Environ. Sci. 7(3): 1134–1141. doi: 10.1039/c3ee43221.

[5] Li H, Chen V. 2010. Membrane Fouling and Cleaning in Food and Bioprocessing. Membrane Technology. 213–254. doi: 10.1016/b978-1-85617-632-3.00010-0.

[6] Goh P, Lau W, Othman M, Ismail A. 2018. Membrane fouling in desalination and its

mitigation strategies. Desalination. 425: 130–155. doi: 10.1016/j.desal.2017.10.018.

[7] Wang X, Lu Z, Jia L, Chen J. 2016. Physical properties and pyrolysis characteristics of rice husks in different atmosphere. Results in Physics. 6: 866–868. doi: 10.1016/j.rinp.2016.09.011. [8] Pareek A, Venkata Mohan S. 2019. Graphene and Its Applications in Microbial Electrochemical Technology. Microbial Electrochemical Technology. 75–97. doi: 10.1016/b978-0-444-64052-9.00004-2.

[9] Hu M, Zheng S, Mi B. 2016. Organic Fouling of Graphene Oxide Membranes and Its Implications for Membrane Fouling Control in Engineered Osmosis. Environmental Science & Technology. 50(2):685–693. doi: 10.1021/acs.est.5b03916.

[10] Cohen-Tanugi D, Grossman JC. 2012. Water Desalination across Nanoporous Graphene. Nano Letters. 12(7): 3602–3608.

[11] Yang Y, Yang X, Liang L, Gao Y, Cheng H, Li X, Zou M, Ma R, Yuan Q, Duan X. 2019. Large-area graphene-nanomesh/carbon-nanotube hybrid membranes for ionic and molecular nanofiltration. Science. 364(6445): 1057–1062.

[12] Abraham J, Vasu KS, Williams CD, Gopinadhan K, Su Y, Cherian CT, Carbone P. 2017. Tunable sieving of ions using graphene oxide membranes. Nature nanotechnology. 12(6): 546.

[13] Li Y, Zhao W, Weyland M, Yuan S, Xia Y, Liu H, Jian M, Yang J, Easton CD, Selomulya C, et al. 2019. Thermally Reduced Nanoporous Graphene Oxide Membrane for Desalination. 53(14): 8314–8323.

[14] Lori J, Lawal A, Ekanem E. 2007. Proximate and Ultimate Analyses of Bagasse, Sorghum and Millet Straws as Precursors for Active Carbons. Journal of Applied Sciences. 7(21): 3249–3255. doi: 10.3923/jas.2007.3249.3255.

[15] Othman N, Hussin MH, Shuib RK, Sulaiman N. 2018. Comparison characteristic between milled coconut shell activated carbon powder and carbon black: Physical, chemical and morphological properties. 1985 (2018).

[16] Supriyanto G, Rukman NK, Nisa AK, Jannatin M, Piere B, Abdullah, Fahmi MZ, Kusuma HS 2018. Graphene Oxide from Indonesian Biomass: Synthesis and Characterization. BioResources. 13(3): 4832–4840.

[17] Habte AT, Ayele DW. 2019. Synthesis and Characterization of Reduced Graphene Oxide (rGO) Started from Graphene Oxide (GO) Using the Tour Method with Different Parameters. Advances in Materials Science and Engineering. 2019: 1–9.

[18] Wenxuan Z, Zhanpeng L, Jing X, Feng L, Wenzhi H, Guangming L, Juwen H. 2017. Frontiers of Environmental Science & Engineering. Preparing graphene from anode graphite of spent lithium-ion batteries. 11(5): 6.

[19] Çiplak, Z, Yildiz N, Çalimli A. 2014. Investigation of graphene/Ag nanocomposites synthesis parameters for two different synthesis methods. Fullerenes, Nanotubes, and Carbon Nanostructures. 23(4): 361–370.

[20] Mayerhöfer TG, Mutschke H, Popp J. 2016. Employing Theories Far beyond Their Limits-The Case of the (Boguer-) Beer-Lambert Law. ChemPhysChem. 17(13): 1948–1955.